

Reversibly Altering Electronic Conduction through a Single Molecule by a Chemical Binding Event

Bala Sundari T. Kasibhatla,[†] André P. Labonté,[‡] Ferdows Zahid,[§] Ronald G. Reifenberger,[‡] Supriyo Datta,[§] and Clifford P. Kubiak^{*,†}

Department of Chemistry & Biochemistry, University of California San Diego, La Jolla, California 92093-0358, Department of Physics, Purdue University, West Lafayette, Indiana 47907, and School of Electrical and Computer Engineering, Purdue University, West Lafayette, Indiana 47907

Received: September 11, 2003

This letter presents experimental evidence that the electrical conductance of a single molecule can be altered by a chemical binding event. Self-assembled monolayers of electron donor tetramethyl xylyl dithiol (TMXYL) have been synthesized and chemically switched to a conducting state by reaction with an electron acceptor tetracyanoethylene (TCNE). Low bias conductance measurements obtained by scanning tunneling spectroscopy under ultrahigh vacuum conditions show a change from insulating to ohmic behavior as a result of the electron donor/acceptor interaction.

Introduction. Self-assembled monolayers (SAMs) of thiols and dithiols on metal and semiconductor surfaces have attracted significant interest because of their potential use in nanoscale functional devices.^{1–5} Electronic conduction through “molecular wires” has been studied^{6–11} and theoretical models have been advanced^{12–20} in attempts to understand electron transport through molecules. These prior studies have demonstrated that the location of the equilibrium Fermi level relative to the HOMO–LUMO gap of a molecule is an important factor in determining the molecular resistance. For the case where the molecule makes a good electrical contact to two electrodes, the resistance could be near $12.9 \text{ K}\Omega$, the quantum of resistance, if the Fermi level is aligned with either the HOMO (or LUMO) of the molecule and the conduction mechanism is ballistic. However, the large resistances measured (on the order of $\text{M}\Omega$)^{12,21,22} clearly indicate that the Fermi level usually lies close to the center of the HOMO–LUMO gap of common unsaturated organic molecules. As a consequence, conduction through the molecule occurs via tunneling.

Here, we report our studies of the structure and electronic properties of SAMs of organic charge-transfer complexes. The formation of a surface-confined charge-transfer complex is accomplished by the reaction of a strong electron acceptor (tetracyanoethylene, TCNE) with a SAM of an electron donor (tetramethyl xylyl dithiol, TMXYL). This reaction results in a 50-fold increase in the conductivity, measured by STM. These results demonstrate that a simple additive chemical reaction can be used to turn on current flow through a molecule by inducing a change from insulating to conducting behavior. These results provide experimental verification of the tuning of a molecular wire junction through appropriate chemistry.²³

Results and Discussion. Organic charge transfer (CT) complexes can be viewed as the result of the reaction of an electron donor molecule (D) with an electron acceptor molecule

TABLE 1: RAIRS Data for the Various SAMs Used in This Study^a

SAM	$\nu(\text{cm}^{-1})$	vibrational mode assignment	RAIRS intensity
TMXYL-Upright, 1	1590	8a , C–C stretch	↑
	1472	19a , C–C stretch	↑
	1439	19b , C–C stretch	↑
	1297	14 , C–C stretch	↑
TMXYL-TCNE, 2	1437	19a , C–C stretch	↓
	1378	CH ₂ out of plane bend	↑
	554	C–CN out of plane bend	↑
TMXYL-Flat, 3	1374	CH ₂ out of plane bend	↑

^a The direction of the arrows in the last column indicates the relative change in intensity of the appropriate spectral bands for selected vibrational modes relative to the bulk (KBr pellet) IR spectrum.

TABLE 2: Ellipsometry and Water Contact Angle Data for Various SAMs Used in This study

SAM	ellipsometry film thickness (nm)	contact angle (θ)
TMXYL-Upright, 1	0.80	80°
TMXYL-TCNE, 2	0.60	71°

(A). TCNE is a relatively strong π -acceptor molecule and readily forms a CT complex with the electron donor, hexamethyl benzene.²⁴ We prepared the dithiol TMXYL^{25,26} because it was expected to possess both the ability to form SAMs and sufficient electron donor character to form an organic CT complex with TCNE. SAMs of TMXYL and TMXYL-TCNE were prepared²⁷ on Au substrates²⁸ and characterized by reflection absorption infrared spectroscopy (RAIRS) (Table 1), ellipsometry (Table 2), electrostatic force microscopy, and contact angle (Table 2) measurements. The characterization of the molecules by these techniques supports the morphology illustrated in Figure 1. The conductance of these SAMs was subsequently investigated by scanning tunneling microscopy (STM) using well-established techniques.²⁹

Properties of a SAM of TMXYL: TMXYL – Upright (1). RAIRS data for **1** (Table 1) suggest that the TMXYL molecule is oriented vertically on Au(111) (Figure 1). This is evident from the increase in the intensity of the infrared (IR) vibrational

* Corresponding author. Telephone: (858) 822-2665. Fax: (858) 534-5383. E-mail: ckubiak@ucsd.edu.

[†] University of California San Diego.

[‡] Department of Physics, Purdue University.

[§] School of Electrical and Computer Engineering, Purdue University.

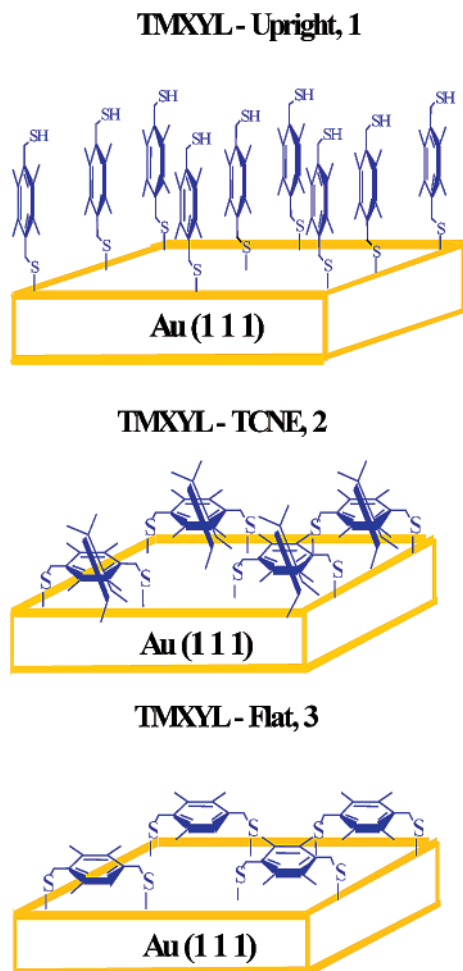


Figure 1. Schematic of the three samples prepared in this study. RAIRS data from TMXYL-upright, **1**, indicates that TMXYL is single-thiol bonded to Au(111) with an upright orientation. The process of reacting TMXYL with TCNE causes the TMXYL to reorient from an upright to a horizontal orientation, indicative of a molecule bonded to the Au(111) substrate via both thiol end-groups. RAIRS confirms that the TMXYL molecules are parallel to the Au(111) surface with the TCNE resting on top. After the TCNE is removed, the TMXYL remains bonded to Au(111) through both thiol groups. Consequently the molecules are parallel to the Au(111) surface. SAMs of **1** were made as a processing step toward SAMs of **2** and **3**.

bands at 1590 cm^{-1} (**8a**) and 1472 cm^{-1} (**19a**). These bands correspond to vibrational modes with a net dipole change that is along the long axis of the TMXYL molecule. Ellipsometry and contact angle measurements are consistent with the proposed vertical orientation of TMXYL (Table 2).

Formation of a Surface Confined Charge-Transfer Complex: TMXYL–TCNE (2). The SAM of **2** was prepared in two steps. The first step was the formation of a SAM of **1** on Au(111) as described above. The second step involved the immersion of the TMXYL coated Au(111) substrate in a concentrated (0.1 M) CH_2Cl_2 solution of TCNE. The RAIRS spectrum of **2** shows an intense band at 1378 cm^{-1} , corresponding to the CH_2 out-of-plane bending mode of TMXYL. In contrast, the in-plane mode at 1437 cm^{-1} (**19b**) decreases significantly in intensity. This suggests that TMXYL is now lying flat with respect to the Au(111) surface, bound through both thiol groups (Figure 1). In addition, the out-of-plane “puckering” mode of TCNE at 554 cm^{-1} shows a significant increase in intensity. These data suggest that TCNE is also lying flat with respect to the metal surface, presumably on top of TMXYL. Ellipsometry and contact angle measurements are

consistent with the proposed horizontal orientation of TMXYL–TCNE **2** (Table 2). In particular, the two-component SAM of TMXYL–TCNE **2** is found by ellipsometry to have a thickness that is 0.2 nm less than that of a SAM of upright TMXYL (**1**) alone.

Properties of a SAM of TMXYL after Removal of TCNE: TMXYL – Flat (3). TCNE was removed from **2** by immersion in a solution of the strong electron donor trimethyl tetrathiafulvalene (Me_3TTF). The RAIRS spectrum of **3** shows the same intense band at 1374 cm^{-1} as seen in the RAIRS of the charge-transfer SAM **2**, suggesting that TMXYL remains flat on Au(111) (Figure 1). The absence of the out-of-plane bending mode at 554 cm^{-1} also confirms the removal of TCNE from the surface. Further support for the surface structures of TMXYL–upright (**1**), the flat sandwich structure of the TMXYL–TCNE CT complex (**2**), and TMXYL–flat (**3**) come from electrostatic force measurements.³⁰

It is useful to compare the scanning tunneling spectra (STS) results obtained from **2** and **3** under identical conditions. The measured conductance near zero bias has two contributions—one due to the tunnel gap between tip and molecule and a second due to a few molecules (perhaps only one) through which the tunneling current must flow. When the tip is brought close to the molecule so as to produce a negligible tunnel gap, the electronic properties of the molecule can dominate the measured $I(V)$. It is important to be in this regime when comparing STS spectra from **2** and **3**.

In this study, this was accomplished by systematically measuring $I(V)$ as a function of set point voltage and current. As the set point voltage is reduced for a fixed tunnel current, the $I(V)$ data becomes reasonably symmetric, indicating that the capacitive coupling between the tip and molecule is comparable to the capacitive coupling between the molecule and the substrate.¹⁷ Under these circumstances (a tunnel resistance of $\sim 1.5\text{ G}\Omega$ for the SAMs investigated here), we have determined that the apex of the tip is close but not buried in the molecular SAM.

With the STM in stable operation under these conditions, the feedback was disabled and the voltage bias between substrate and tip was ramped, generating $I(V)$ data at 256 different values of the bias voltage. Under ideal circumstances, when $I(V)$ data are acquired as described above, the resulting tunnel gap between tip and molecule should be identical for both **2** and **3**. Thus, any observed changes in the $I(V)$ can be interpreted as changes in molecular conductance, a quantity of considerable interest. Under actual operating conditions, to achieve a given set point, the tip–molecule separation is greater for a more conducting molecule. Since **2** is found to be more conductive than **3**, it follows that differences observed in $I(V)$ (or dI/dV) near zero bias will tend to underestimate the actual differences in the conductance between the two molecular SAMs under investigation.

A comparison of the STM data for **2** and **3** provides important information about the molecular electronic effects induced by the formation of a charge-transfer complex. The $I(V)$ data are shown in Figure 2. The data were taken at $V_{\text{set}} = -1.5\text{ V}$ and $I_{\text{set}} = -1.0\text{ nA}$. STM $I(V)$ data for **2** clearly show ohmic behavior for $|V| \leq 0.5\text{ V}$, indicating that the TMXYL–TCNE CT complex has a very different electronic behavior compared to **3** (TMXYL–flat).

The change from insulating to conducting behavior at low bias by the addition of TCNE is most clearly seen by a direct comparison of dI/dV . $\text{Log}_{10}(dI/dV)$ derived from representative

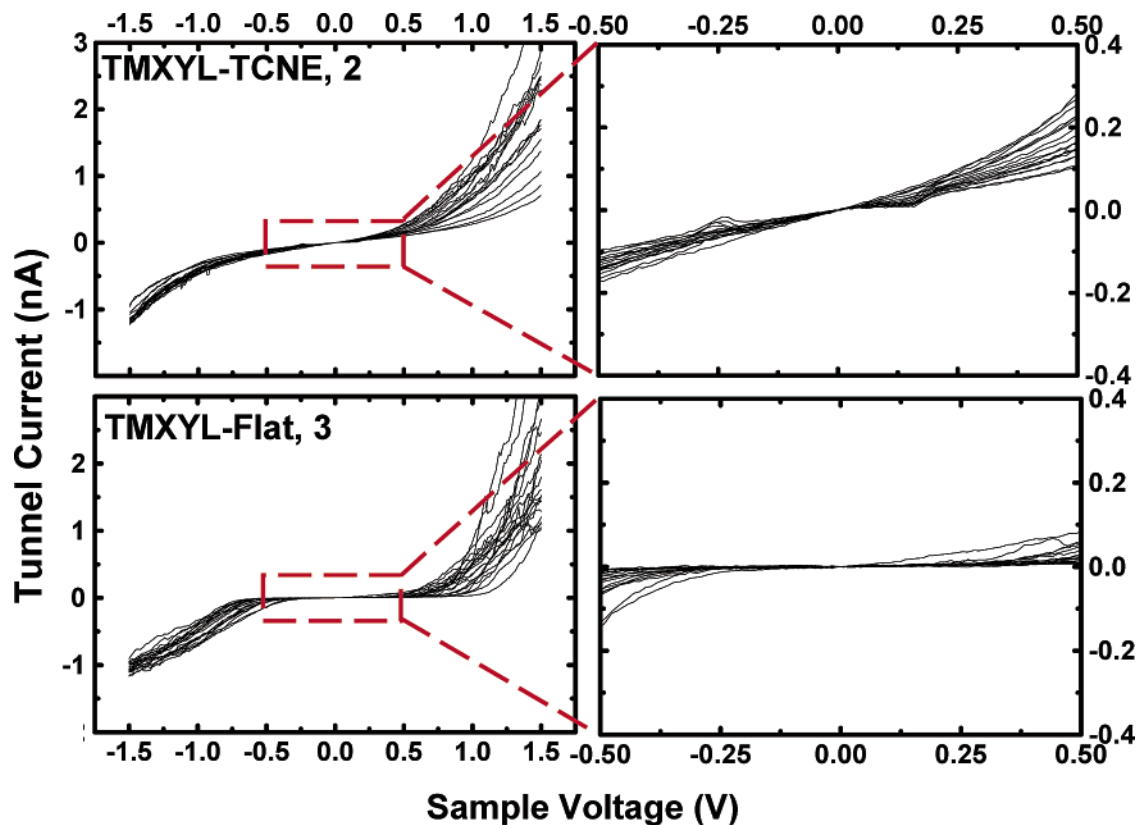


Figure 2. $I(V)$ data from **2** indicates that the CT complex is an electrical conductor, with a nearly linear $I(V)$ behavior at $V = 0$. When the TCNE molecule is removed, $I(V)$ data from **3** indicate that for small voltages ($|V| < 0.5$ V) TMXYL is an electrical insulator. These data combined with the $I(V)$ data on TMXYL–TCNE indicate that the change from insulator to conductor through the formation of a CT complex results from a change in the molecular energy levels. Approximately 25 separate $I(V)$ spectra, taken from various regions across the sample, are plotted simultaneously to indicate the overall reproducibility of the data. The data have been reproduced on two separate SAMs.

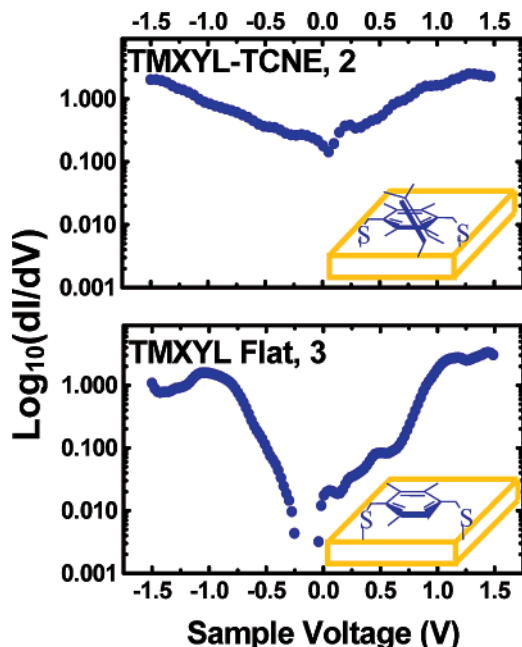


Figure 3. $\text{Log}_{10}(dI/dV)$ data for TMXYL–TCNE, **2**, and TMXYL–flat, **3**. The dI/dV were calculated from a representative $I(V)$ shown in Figure 2. The units of dI/dV are nA/V. Near zero bias, **2** is found to be approximately 50 times more conductive than **3**.

$I(V)$ data of **2** and **3** are shown in Figure 3. The data show that the zero-bias conductivity of **2** is a factor of at least 50 greater than that of **3**. In comparing the relative conductivity of **2** and **3** at 0.01 nA/V (the estimated noise level of our system), we find that **3** exhibits a conduction gap while **2** does not.

It is useful to assess the change in conductivity resulting from the structural change of the TMXYL molecule on the metal surface between **1** and **3**. We therefore examined a SAM of TMXYL–upright, **1** (see Figure 1). $I(V)$ data for **1** indicate insulating behavior with little conduction evident for $|V| \leq 1.0$ V. However, **3** appears somewhat less insulating than **1**, presumably because SAM **3** is not as thick. The relatively small difference in conductivity of **1** and **3** is attributed to the orientation change of the molecule from vertical (**1**) to horizontal (**3**). However, the TMXYL molecules in **2** and **3** share similar physical orientations but conduct quite differently. Consequently, the change from the Ohmic behavior observed for **2** to the insulating behavior observed for **3** results from the removal of the electron acceptor, TCNE. The removal of TCNE eliminates the CT interactions, which returns insulating properties to the SAM. This behavior is completely reversible. Thus, a flattened SAM of TMXYL (**3**) can be reimmersed into a solution of TCNE and the spectroscopic and conductive properties of TMXYL–TCNE (**2**) are restored.

The evidence for Ohmic conduction in the TMXYL–TCNE CT monolayer **2** is compelling and indicates that **2** has energy states near the Fermi energy. The clear difference between the $I(V)$ of **2** and **3** demonstrates that a change in the conductance of the TMXYL is due to the creation of the TMXYL–TCNE CT complex and not due to the change in morphology. An energy diagram consistent with these observations is provided in Figure 4. This energy diagram is obtained using the DFT method, B3PW91 with 6-31G* basis function as implemented in the chemistry software Gaussian 98.³¹ This method (B3PW91) combines the Becke exchange functional³² and the Perdew–Wang correlation functional.³³ Figure 4 shows the energy levels

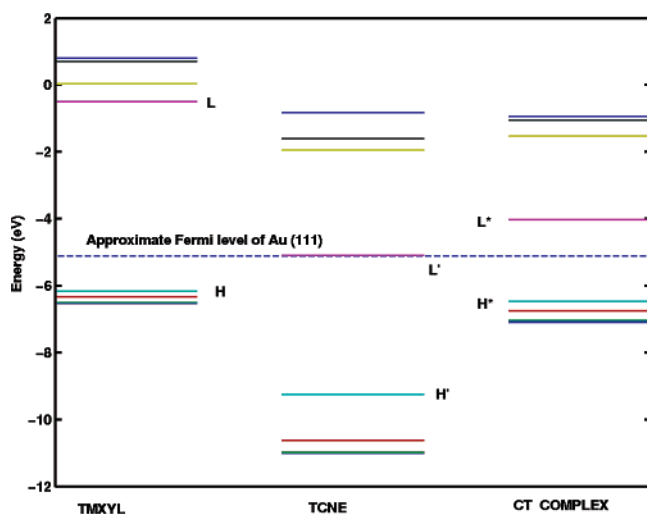


Figure 4. Energy levels of TMXYL and TCNE molecules along with those of CT complex. This result is obtained from B3PW91 method with 6-31G* basis using Gaussian 98. Approximate Fermi level (-5.1 eV) of Au(111) is indicated with broken line.

of TMXYL and TCNE molecules along with those of the CT complex. The CT complex is modeled by placing TCNE on top of TMXYL at a distance of 0.285 nm. The substrate Fermi level can be assumed to be located around -5.1 eV (work function of bulk gold), although a more detailed calculation is needed to locate it precisely with respect to the molecular levels. The point to note is that the CT complex gives rise to an additional hybridized level (L^*) close to the Fermi level, leading to an increase in the density of states. This increase in the density of states contributes to increased conduction since this level is delocalized; that is, it hybridizes with the substrate through the sulfur atoms of TMXYL. This simple physical picture provides a mechanism for an important capability in molecular electronics, the ability to alter the electronic properties of an individual molecule by a molecular binding process. Changes in conductance of chemical nanostructures that occur in response to a pH change³⁴ or redox reaction³⁵ have been reported previously. The large change in conductivity that follows the chemical formation of the TMXYL–TCNE CT complex appears to occur by a different mechanism involving the rehybridization of molecular energy levels. The overall effects of tuning energy levels by field effect transistor (FET)-like behavior vs chemical bond formation were recently considered theoretically.²³ Both can alter conduction by moving the poles of the molecular Green's function in a Landauer treatment.

Conclusions. Self-assembled monolayers of the dithiol TMXYL were synthesized on a Au(111) substrate. The addition of the electron acceptor, TCNE, caused a charge-transfer complex of TMXYL with TCNE to be formed. The surface morphology of the SAMs was characterized by reflection absorption infrared spectroscopy, ellipsometry, electrostatic force microscopy,³⁰ and contact angle measurement. $I(V)$ data obtained in UHV by an STM revealed a significant change in the conductance spectra between the TMXYL and TMXYL–TCNE SAMs. SAMs formed from TMXYL alone produced $I(V)$ data similar to that reported elsewhere for poly(phenylene) thiols.³⁶ The magnitude of the measured energy gap in the conductance spectra places the HOMO of TMXYL (level H in Figure 4) approximately 1 eV below E_F of Au(111), a result consistent with the calculated energy levels presented here. Upon addition of TCNE, a considerable change in the conductance spectra occurred, resulting in $I(V)$ data that were nearly Ohmic near $V = 0$ and showed no evidence of a gap in the conductivity.

This result is consistent with the introduction of CT complex hybridized level (L^*) that lies near the Fermi level of the substrate (see Figure 4). Upon removal of the TCNE molecule, the insulating character of the self-assembled monolayer was essentially restored.

The significance of this experiment is the clear demonstration that the conductance of an individual molecule can be altered in a controlled and reversible manner. This establishes the feasibility of using current flow through a suitably designed SAM as a sensitive means of detecting the presence (or absence) of a specific target molecule. It is not possible in general to dope individual molecules to levels of small partial charge, as is commonly practiced with semiconductors and conducting polymers to achieve specific conductivities. However, the large and reversible change in conductivity of individual molecules demonstrated for the TMXYL–TCNE system suggests a new molecular technology for fabricating conductive elements useful in future molecular electronic applications.

Acknowledgment. The authors thank T. Lee, S. Howell, R.P. Andres, and D. B. Janes for stimulating discussions throughout the course of this work. This work was supported by an ARO AASERT Grant to augment contract DAAL03-G-0144 and an ARO/NSF Grant DMR-9708107.

References and Notes

- (1) Bains, C. D.; Whitesides, G. M. *Angew. Chem., Int. Ed. Engl.* **1989**, *28*, 506.
- (2) Bain, C. D.; Troughton, E. B.; Tao, Y. T.; Evall, J.; Whitesides, G. M.; Nuzzo, R. G. *J. Am. Chem. Soc.* **1989**, *111*, 321.
- (3) Reed, M. A.; Zhou, C.; Muller, C. J.; Burgin, T. P.; Tour, J. M. *Science* **1997**, *278*, 252.
- (4) Metzger, R. M. *Acc. Chem. Res.* **1999**, *32*, 950.
- (5) Lee, T.; Liu, J.; Dicke, J.; Andres, R. P.; Lauterback, J.; Melloch, M. R.; McInturff, D.; Woodall, J. M.; Reifengerger, R. *Appl. Phys. Lett.* **1999**, *74*, 2869.
- (6) Collard, D. M.; Fox, M. A. *Langmuir* **1991**, *7*, 1192.
- (7) Hickman, J. J.; Labinis, P. E.; Auerbach, D. I.; Zou, C.; Gardner, T. J.; Whitesides, G. M.; Wrighton, M. S. *Langmuir* **1992**, *8*, 357.
- (8) Biebuyck, H. A.; Whitesides, G. M. *Langmuir* **1993**, *9*, 1766.
- (9) Bumm, L. A.; Arnold, J. J.; Cygan, M. T.; Dunbar, T. D.; Burgin, T. P.; Jones, L., II; Allara, D. L.; Tour, J. M.; Weiss, P. S. *Science* **1996**, *271*, 1705.
- (10) Kergueris, C.; Bourgoin, J. P.; Palacin, S.; Esteve, D.; Urbina, C.; Magoga, M.; Joachim, C. *Phys. Rev.* **1999**, *B59*, 12505.
- (11) Wold, D. J.; Frisbie, C. D. *J. Am. Chem. Soc.* **2000**, *122*, 2971.
- (12) Datta, S. *Electronic Transport in Mesoscopic Systems*, Cambridge University Press: Cambridge, 1995.
- (13) Samanta, M. P.; Tian, W.; Datta, S.; Henderson, J. I.; Kubiak, C. P. *Phys. Rev.* **1996**, *B53*, R7626.
- (14) Joachim, C.; Vinuesa, J. F. *Europhys. Lett.* **1996**, *33*, 635.
- (15) Mujica, V.; Kemp, M.; Roitberg, A.; Ratner, M. A. *J. Chem. Phys.* **1996**, *104*, 7296.
- (16) Hsu, C. P.; Marcus, R. A. *J. Chem. Phys.* **1997**, *106*, 584.
- (17) Datta, S.; Tian, W.; Hong, S.; Reifengerger, R.; Henderson, J. I.; Kubiak, C. P. *Phys. Rev. Lett.* **1997**, *79*, 2530.
- (18) Emberly, E.; Kirczenow, G. *Nanotechnology* **1999**, *10*, 285.
- (19) Ventra, M. D.; Pantelides, S. T.; Lang, N. D. *Phys. Rev. Lett.* **2000**, *84*, 979.
- (20) Onipko, A. I.; Berggren, K. F.; Klymenko, Y. O.; Malysheva, L. I.; Rosink, J. J. W. M.; Geerlings, L. J.; van der Drift, E.; Radelaar, S. *Phys. Rev.* **2000**, *61*, 11118.
- (21) Dorogi, M.; Gomez, J.; Osifchin, R. G.; Andres, R. P.; Reifengerger, R. *Phys. Rev.* **1995**, *B52*, 9071.
- (22) Andres, R. P.; Bein, T.; Dorogi, M.; Feng, S.; Henderson, J. I.; Kubiak, C. P.; Mahoney, W.; Osifchin, R. G.; Reifengerger, R. *Science* **1996**, *272*, 1323.
- (23) Mujica, V.; Nitzan, A.; Datta, S.; Ratner, M. A.; Kubiak, C. P. *J. Phys. Chem. B* **2003**, *107*, 91.
- (24) Briegleb, G. *Elektronen-Donator-Acceptor Komplexe*; Springer-Verlag: Berlin, 1961.
- (25) Synthesis of 2,3,5,6-tetramethyl-*p*-xylene- α, α' dithiol (TMXYL, 1): TMXYL was synthesized by modification of existing procedure.²⁶ 2,3,5,6-tetramethyl-*p*-xylene- α, α' -diol (5.5 g; 0.028 mol) was placed in a three-necked, 100 mL flask along with 70 mL acetonitrile. The solid was

dissolved with heating and stirring, followed by the addition of thiourea (4.3 g; 0.056 mol) and approximately 40 mL water. Next aqueous 48 wt % HBr (28.1 g; 0.169 mol) was added to the solution, which was then refluxed, with stirring, for 30–36 h. To the reaction mixture, 67 mL of 2.5 M aqueous KOH was added, and the mixture refluxed for 12 h under nitrogen. It was then allowed to cool to room temperature, whereupon a pale yellow solid precipitated. The solid was dissolved in CHCl_3 , dried over anhydrous MgSO_4 , and solvent removed under reduced pressure. The solid was then loaded on a silica gel column (60–200 mesh) and eluted with a 9:1 mixture of hexanes: EtOAc to obtain 4.52 g (71% yield) of a white crystalline material. IR (KBr): $\nu(\text{SH})$, 2549 cm^{-1} (weak). $^1\text{H NMR}$ (CDCl_3): 1.52 ppm (t, 2H), 2.3 ppm (s, 12H), 3.8 ppm (d, 4H). $^{13}\text{C NMR}$ (CDCl_3): 16.2 ppm, 24.3 ppm, 132.3 ppm, 136.3 ppm. MS: 226 (M+), 193 (M - SH), 161. C, H, N (vs *calcd.*): 63.68% C (63.66%), 8.00% H (8.00%), 28.22% S (28.32%).

(26) Rohrbach, W. D.; Boekelheide, V. *J. Org. Chem.* **1983**, *48*, 3673.

(27) A SAM of TMXYL (Figure 1) was prepared by immersing a clean Au(111) wafer into ca. 1 mM CH_2Cl_2 solutions of the respective compound for 12–16 h. The wafers were then thoroughly rinsed with CH_2Cl_2 and dried overnight under a stream of nitrogen. A SAM of TMXYL–TCNE, **2**, was prepared by immersing a Au(111) wafer previously coated with **1**, in a concentrated solution of TCNE in CH_2Cl_2 for 48 h. The wafer was rinsed with CH_2Cl_2 and dried under nitrogen. A SAM of TMXYL with two thiol bonds to the Au(111) surface, **3**, was prepared by immersing the TMXYL–TCNE SAM, **2**, in a concentrated solution of trimethyltetra-thiafulvalene (Me_3TTF) in CH_2Cl_2 for 30 h.

(28) All RAIRS substrates consist of a layer of Cr (1–4 nm) and Au (200–300 nm) evaporated onto a borosilicate glass. Before use, all Au substrates are front-side flamed until bright red for 30 to 40 s, producing atomically flat grains of a few microns in diameter with a Au(111) orientation. Just prior to use, all wafers were rinsed in distilled ethanol to remove residual contamination.

(29) An ultrahigh vacuum (UHV) scanning tunneling microscope (STM) was used to take topography and conductance spectra of SAMs. The STM is housed in a stainless steel chamber pumped to a pressure of better than 1×10^{-9} Torr. When performing STM studies of SAM-covered surfaces, precautions must be taken to ensure the tip is not buried in the SAM layer. For the results reported below, this was accomplished by monitoring the noise in the z -piezo feedback voltage and tunnel current during STM topographic scans. Each $I(V)$ data curve plotted is an average of forty individual voltage sweeps taken in quick succession.

(30) Howell, S.; Kuila, D.; Kasibhatla, B.; Kubiak, C. P.; Janes, D.; Reifenberger, R. *Langmuir* **2002**, *18*, 5120.

(31) Frisch, M. J.; Trucks, G. W.; Schlegel, H. B.; Scuseria, G. E.; Robb, M. A.; Cheeseman, J. R.; Zakrzewski, V. G.; Montgomery, J. A., Jr.; Stratmann, R. E.; Burant, J. C.; Dapprich, S.; Millam, J. M.; Daniels, A. D.; Kudin, K. N.; Stains, M. C.; Farkas, O.; Tomasi, J.; Barone, V.; Cossi, M.; Cammi, R.; Mennucci, B.; Pomelli, C.; Adamo, C.; Clifford, S.; Ochterski, J.; Petersson, G. A.; Ayala, P. Y.; Cui, Q.; Morokuma, K.; Malick, D. K.; Rabuck, A. D.; Raghavachari, K.; Foresman, J. B.; Cioslowski, J.; Ortiz, J. V.; Baboul, A. G.; Stefanov, B. B.; Liu, G.; Liashenko, A.; Piskorz, P.; Komaromi, I.; Gomperts, R.; Martin, R. L.; Fox, D. J.; Keith, T.; Al-Laham, M. A.; Peng, C. Y.; Nanayakkara, A.; Gonzalez, C.; Challacombe, M.; Gill, P. M. W.; Johnson, B.; Chen, W.; Wong, M. W.; Andres, J. L.; Gonzalez, C.; Head-Gordon, M.; Replogle, E. S.; Pople, J. A. *Gaussian 98, Revision A.7*; Gaussian, Inc.: Pittsburgh, PA, 1998.

(32) Becke, A. D. *J. Chem. Phys.* **1993**, *98*, 5648.

(33) Perdew, J. P.; Wang, Y. *Phys. Rev.* **1992**, *B45*, 13244.

(34) Brousseau, L. C., III.; Zhao, Q.; Shultz, D. A.; Feldheim, D. L. *J. Am. Chem. Soc.* **1998**, *120*, 7645.

(35) Gittins, D. I.; Bethell, D.; Schiffrin, D. J.; Nichols, R. J. *Nature* **2000**, *408*, 67.

(36) Hong, S.; Tian, W.; Henderson, J.; Datta, S.; Kubiak, C. P.; Reifenberger, R. *Superlattices Microstruct.* **2000**, *28*, 289.